Discontinuous Galerkin Method Based on Quadrilateral Mesh for Maxwell's Equations

Misun Min
Mathematics and Computer Science Division, Argonne National Laboratory
Argonne, IL, 60439 USA
mmin@mcs.anl.gov

Abstract: Discontinuous Galerkin (DG) methods based on quadrilateral spectral element discritizations are applied to the eletromagnetic wave time-domain simulations in free space. The 2D Maxwell's equations in transverse-magnetic mode are described in conservation form. Numerical flux is used for the communication at the interface between elements and boundary condition. Computational results on the field distribution are demonstrated, including h- and p-convergence in maximum norm with this method. This work is our first step toward two- and three-diemensional nanophotonic simulations using this higher order method.

Keywords. Discontinuous Galerkin method, spectral element discritizations

1. Formulation

Consider the two-dimensional Maxwell's equations in transverse-magnetic (TM) mode, which expresses the electromagnetic field vectors by decomposing each component as follows:

$$H = (H_x, H_y, 0), \quad \text{and} \quad E = (0, 0, E_z). \tag{1}$$

Then the governing equations are

$$\frac{\partial q}{\partial t} = A\frac{\partial q}{\partial x} + B\frac{\partial q}{\partial y}, \tag{2}$$

where the field vector is $q = [H_x, H_y, E_z]^T$ and the coefficient matrices are

$$A = \begin{bmatrix} 0 & 0 & 0 \\ 0 & 0 & -\frac{1}{\mu} \\ 0 & -\frac{1}{\epsilon} & 0 \end{bmatrix}, B = \begin{bmatrix} 0 & 0 & \frac{1}{\mu} \\ 0 & 0 & 0 \\ \frac{1}{\epsilon} & 0 & 0 \end{bmatrix}. \tag{3}$$

Writing the equation (2) in conservation form [2], [3], we have

$$Q\frac{\partial q}{\partial t} + \nabla \cdot F(q) = 0, \tag{4}$$

where Q represents the materials, q the field vector, and $F(q)$ the flux, defined by

$$Q = \begin{bmatrix} \mu & 0 & 0 \\ 0 & \mu & 0 \\ 0 & 0 & \epsilon \end{bmatrix}, q = \begin{bmatrix} H_x \\ H_y \\ E_z \end{bmatrix}, F(q) = \begin{bmatrix} 0 & -E_z \\ E_z & 0 \\ H_y & -H_x \end{bmatrix}^T. \tag{5}$$

In the general case of materials with finite conductivity, no surface charges and currents can exist, and simplified conditions take the form that, along the interface of any two dielectric bodies, endowed with an outward pointing normal vector, $\hat{n}$, the tangential field components remain contiuous, that is,

$$\hat{n} \times \|E\| = 0, \;\; \hat{n} \times \|H\| = 0, \tag{6}$$

where

$$\|u\| = u^+ - u^- \tag{7}$$

represents the jump in field value across the interface, with u^+ representing the neighboring field value and u^- the local field value.

2. Weak Formulation

Assume that our computational domain is Ω. In each element, we seek the local solution q_N in an admissible space, to be defined later, satisfying

$$\left(Q\frac{\partial q_N}{\partial t} + \nabla \cdot F(q_N), \phi\right)_{\Omega^e} = 0. \tag{8}$$

where ϕ is a local discontinuous test function. Integrating by parts of (8), we obtain

$$\left(Q\frac{\partial q_N}{\partial t}, \phi\right)_{\Omega^e} - (\hat{n} \cdot F(q_N), \nabla \cdot \phi)_{\Omega^e} = -(\hat{n} \cdot F(q_N), \phi)_{\partial\Omega^e}. \tag{9}$$

However, neighboring elements will share some part of the local element boundary, $\partial\Omega^e$. Thus, at this point we will have two solutions, and we must choose one, or a combination of the two, that is correct. To this end we define a numerical flux F^* and replace the right-hand side of (9), F by $F*$,

$$\hat{n} \cdot F^* = \hat{n} \cdot F^*(q^-, q^+), \tag{10}$$

where q^- refers to the local solution and q^+ the solution in the neighboring elements. With the numerical flux F^* to connect the elements, we integrate by parts once more for equation (9) and get the final form

$$\left(Q\frac{\partial q_N^-}{\partial t} + \nabla \cdot F(q_N^-), \phi\right)_{\Omega^e} = \left(\hat{n} \cdot [F(q_N^-) - F^*(q_N^-, q_N^+)], \phi\right)_{\partial\Omega^e}. \tag{11}$$

There are several possible of choices for this flux function. Here we choose the upwinding flux [2], [3], [5]:

$$\hat{n} \cdot F^*(q^-, q^+) = \frac{1}{2}\left\{ \begin{array}{c} \bar{Y}^{-1}\hat{n} \times (-Y^+\|E\| - \hat{n} \times \|H\|) \\ \bar{Z}^{-1}\hat{n} \times (Z^+\|H\| - \hat{n} \times \|E\|) \end{array} \right., \tag{12}$$

where $\|E\| = E^+ - E^-$ and $\|H\| = H^+ - H^-$, and the local impedence Z^-, conductance Y^- (neighboring the material properties Z^+, conductance Y^+), and their average values are given by

$$Z^\pm = \sqrt{\frac{\mu^\pm}{\epsilon^\pm}}, \;\; Y^\pm = \sqrt{\frac{\epsilon^\pm}{\mu^\pm}}, \;\; \bar{Z} = \frac{Z^+ + Z^-}{2} \;\text{ and }\; \bar{Y} = \frac{Y^+ + Y^-}{2}. \tag{13}$$

For simplicity, we solve the problem for the case with $\mu = \epsilon = 1$ everywhere in the domain. In the case, we have $Z^{\pm} = Y^{\pm} = \hat{Z} = \hat{Y} = 1$, so that the penalizing boundary term is the following:

$$\hat{n} \cdot F^*(q^-, q^+) = \frac{1}{2} \begin{cases} \hat{n} \times (-\|E\| - \hat{n} \times \|H\|) \\ \hat{n} \times (\|H\| - \hat{n} \times \|E\|) \end{cases} . \tag{14}$$

Applying $\hat{n} \times (\hat{n} \times E) = \hat{n}(\hat{n} \cdot E) - (\hat{n} \cdot \hat{n})E$ to (14), we get the detailed expression for the flux:

$$\hat{n} \cdot (F - F^*)(q^-, q^+) = \frac{1}{2} \begin{cases} -n_y\|E_z\| - n_x(n_x\|H_x\| + n_y\|H_y\|) + \|H_x\| \\ n_x\|E_z\| - n_y(n_x\|H_x\| + n_y\|H_y\|) + \|H_y\| \\ n_x\|H_y\| - n_y\|H_x\| + \|E_z\| \end{cases} . \tag{15}$$

3. Numerical Scheme

We seek the local solution

$$q_N^e(x_i^e, t) = \sum_{j=0}^{N} q_j^e(t) l_j(x_i^e) = \sum_{j=0}^{N} \hat{q}_j^e(t) \Phi_j(x_i^e), \tag{16}$$

where $l_j(x^e)$ is the local Lagrangian basis in P_N^2, $\Phi_j(x^e) \in P_N^2$ is the orthonormal Legendre basis, and x_j^e are predefined N local grid-points. Define the multidimensional Vandemonde matrix, V, by

$$V_{ij} = \Phi_j(x_i^e), \tag{17}$$

where P_j is the multivariate Legendre polynomial of degree j. Since

$$\begin{bmatrix} \Phi_0(x^e) \\ \vdots \\ \Phi_N(x^e) \end{bmatrix} = \begin{bmatrix} \Phi_0(x_0^e) & \cdots & \Phi_0(x_N^e) \\ \vdots & \cdots & \vdots \\ \Phi_N(x_0^e) & \cdots & \Phi_N(x_N^e) \end{bmatrix} \begin{bmatrix} l_0(x^e) \\ \vdots \\ l_N(x^e) \end{bmatrix}, \tag{18}$$

one can represent the Lagrange polynomials evaluated at x^e as

$$l^e(x^e) = (V^T)^{-1}\Phi(x^e). \tag{19}$$

Then the semidiscrete scheme of equation (11) with an identity matrix Q is

$$M\frac{dq_N}{dt} + S \cdot F(q_N) = F\left(\hat{n} \cdot [F_N - F*]\right), \tag{20}$$

where

$$M_{ij} = (l_i, l_j)_\Omega, S_{ij} = (l_i, \nabla l_j)_\Omega, F_{ij} = (l_i, l_j)_{\partial\Omega}. \tag{21}$$

The final form of the semidiscrete scheme (20) is

$$\frac{d(H_x)_N}{dt} - M^{-1}S_y(E_z)_N = M^{-1}F\left(-n_y\|E_z\| - n_x(n_x\|H_x\| + n_y\|H_y\|) + \|H_x\|\right) \tag{22}$$

$$\frac{d(H_y)_N}{dt} + M^{-1}S_x(E_z)_N = M^{-1}F\left(n_x\|E_z\| - n_y(n_x\|H_x\| + n_y\|H_y\|) + \|H_y\|\right) \tag{23}$$

$$\frac{d(E_z)_N}{dt} + M^{-1}\left(S_x(H_y)_N - S_y(H_x)_N\right) = M^{-1}F\left(n_x\|H_y\| - n_y\|H_x\| + \|E_z\|\right). \tag{24}$$

For the time integration, we use the forth-order Runge-Kutta scheme.

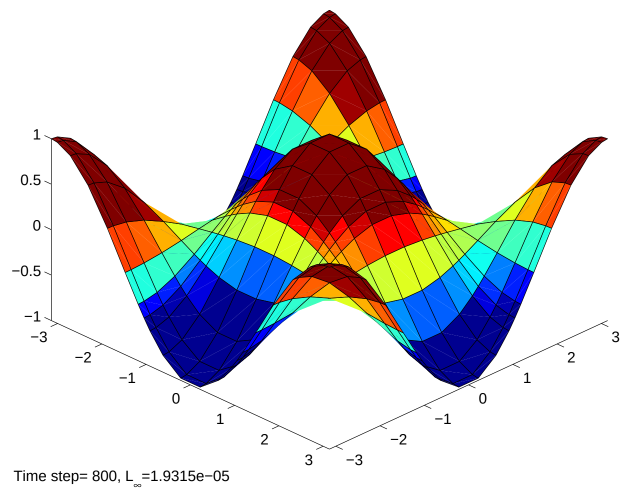

Figure 1: Field distribution of E_z after 3 periods in time: The number of nodes in one subdomain = 8×8; in 9 elements, $\Delta t = 0.016$.

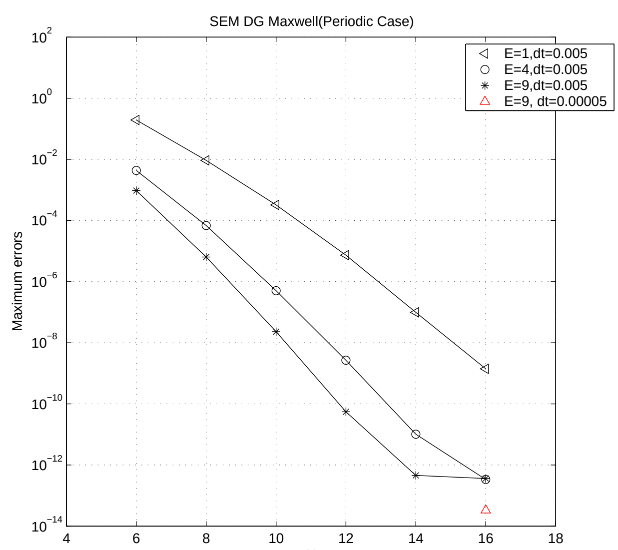

Figure 2: (b) p–convergence and h–convergence: E is the number of elements, N is the number of grids on a face, and dt(=Δt) is the time step size.

4. Computational Results

The computational results for the 2D Maxwell's equations in TM mode with periodic boundary condition are demonstrated. For a domain $[-\pi,\pi]^2$, the analytic solutions are

$$H_x = \cos(x)\sin(y)\sin(\sqrt{2}t)/\sqrt{2}, \quad (25)$$

$$H_y = -\sin(x)\cos(y)\sin(\sqrt{2}t)/\sqrt{2}, \quad (26)$$

$$E_z = \cos(x)\cos(y)\cos(\sqrt{2}t). \quad (27)$$

Figure 1 shows the field distribution of E_z after 3 periods time with a time step size $\Delta t = 0.016$. The domain is equally subdivided into 9 elements with the number of the nodes on the face, $N = 8$. In the case, the maximum error shows 4 digits accuracy. Figure 2 shows the maximum errors depending on the mesh refinement and the degree of polynomials for the approximation with a fixed time step size Δt. The errors show high-order convergence. Note that, in the case of $N = 16$ with 9 elements, time error from fourth-order Runge-Kutta method dominates when $\Delta t = 0.005$. However, reducing the time step size by $\Delta t = 0.00005$, one can observe that spatial error dominates again to confirm high order convergence.

5. Conclusions

We have discussed the formulation of a discontinuous Galerkin scheme based on quadrilateral mesh and shown some primary results on the convergence of the method for 2D Maxwell's equations. The computational results show that the scheme is high-order accurate and efficient. The discontinuous formulations with this method will render similar performace for the problems involving nonsmoothness. We remain the implementation of this method to a nanophotonic problem [4] as future work.

Acknowledgement

This work was supported by the Mathematics, Information, and Computational Science Division subprogram of the Office of Advanced Scientific Computing Research, Office of Science, under DOE contract W-31-109-ENG-38.

References

[1] M. O. Deville, P. F. Fischer, E. H. Mund, High-order methods for incompressible fluid flow, Cambridge University Press, Cambridge, UK, 2002.

[2] J. S. Hesthaven, T. C. Warburton, Nodal high-order methods on unstructured grids. I. time-domain solution of Maxwell's equations, Journal of Computational Physics, 181, no. 1, pp. 186–221, 2002.

[3] J. S. Hesthaven, T. Warburton, Higher order nodal discontinuous Galerkin methods for the Maxwell eigenvalue problem, preprint, 2003.

[4] M. S. Min, T. W. Lee, P. F. Fischer, S. K. Gray, Fourier spectral simulations and Gegenbauer reconstructions for electromagnetic waves in the presence of a metal nanoparticle, preprint, 2004.

[5] A.H. Mohammadian, V. Shankar, W.F. Hall, Computation of electromagnetc scattering and radiation using a time-domain finite-volume discretization procedure, Comput. Phys. Comm., 68, pp. 175–196, 1991.